Assessment of AUSMD for Simulating Hypersonic Flowfield with Equilibrium Gas Effects

S. Mostafa Hosseinalipour[1], Hadi Vafadar Moradi[2]

1- Assistant professor, Iran University of Science and Technology, Narmak, Tehran

2- MSc., Iran University of Science and Technology

Abstract

The numerical schemes for hypersonic flow simulation require robustness, accuracy and efficiency. Hypersonic flow problems intrinsically have severe viscous dissipation in a boundary layer and strong shock waves and high enough temperature to violate perfect gas law. For this reason numerical simulations of hypersonic flow problems have obstacles such as the presence of excessive numerical dissipation near a wall and numerical oscillation behind strong shock waves. Today, upwind schemes are main spatial discretization schemes. In this paper first order upwind biased schemes called AUSMD is applied to solve hypersonic flowfields governed by the full Navier-Stokes equations with equilibrium gas effects and formulation required to applied these on structured, unstructured grid types are developed. Three test cases are studied; hypersonic flow with equilibrium gas effects over flat plate, wedge and blunt body to assessed their capabilities in hypersonic flowfields with equilibrium gas effects. Finally results obtained for these test cases are compared with validated references. It will be shown that this scheme is very robust in computing flow properties in the boundary layer region.

Keywords: Hypersonic Flow, Equilibrium Gas, Upwind, AUSMD, Structured and Unstructured Grid

Introduction

With the practical need for efficient hypersonic vehicle design, there has been continuous research to unveil the physics of hypersonic flows experimentally or numerically [1]. The numerical scheme for hypersonic flow simulation requires robustness, accuracy and efficiency. Hypersonic flow problems intrinsically have severe viscous dissipation in a boundary layer and strong shock waves. For this reason numerical simulation of hypersonic flow problems have obstacles such as the presence of excessive numerical dissipation near a wall and numerical oscillations behind strong shock waves [2].

Today, upwind-biased schemes are the main trend of spatial discretization, which may be categorized as either FVS (flux vector splitting) or FDS (flux difference splitting). FVS, such as Steger–Warming's [3] or Van Leer's [4], has advantages in view of robustness and efficiency. It can be proved that these types of FVS schemes are positively conservative under a CFL-like condition [5], which is very desirable for simulating high-speed flows involving strong shocks and expansions. However, it is also well known that these schemes have accuracy problems in resolving shear layer regions due to excessive numerical dissipation, which occurs more seriously in hypersonic flow. Much effort has spent on developing improved FVS-type schemes for high-speed flows, and they have shown reasonable enhancement in accuracy. In contrast, FDS, which exploits the solution of the local Riemann problem, usually provides accurate solutions. Roe's FDS [6] has a matrix that becomes zero at a sonic transition point and a contact discontinuity. Thus it is able to capture a shock and resolve the shear layer region very accurately. Unfortunately, it has several robustness problems such as the violation of the entropy condition, failure of local linearization, and appearance of carbuncles [7]. Those defects become more serious in hypersonic flow than in subsonic or supersonic flow. Although an entropy fix may enhance the robustness, a large amount of entropy fix is usually required in hypersonic flow, which requires extra numerical dissipation. This also may cause a decrease of the total enthalpy behind a shock wave and the inaccurate estimation of the surface heating rate. Determining the optimal amount of entropy fix without compromising accuracy is difficult and depends highly on the user's experience. Some variants of Roe's FDS such as Harten–Lax–van Leer's (HLLE) [8] increase the robustness of Roe's FDS at the expense of accuracy. Therefore, contemporary concern is shifted toward combining the accuracy of FDS and the robustness of FVS.

In an effort to design a numerical scheme to meet this concern, the AUSM (advection upstream splitting method) [9] was proposed by Liou and Steffen. In AUSM a cell-interface advection Mach number is appropriately defined to determine upwind extrapolation for convective quantities. As a result, AUSM is

1- Assistant professor, Iran University of Science and Technology

2- MSc., Research assistant, Iran University of Science and Technology accurate enough to resolve a shear layer, and it is simple and robust. Thus AUSM possesses the merits suitable for the analysis of hypersonic flows. In this paper one of the AUSM based scheme called AUSMD is used to assess its capabilities in hypersonic flow fields with equilibrium gas effects.

Governing Equations

The 2D Navier–Stokes equations in a conservation form can be expressed as:

$$\frac{\partial \vec{Q}}{\partial t}+\frac{\partial \vec{E}}{\partial x}+\frac{\partial \vec{F}}{\partial y}=\left(\frac{\partial \vec{E}_v}{\partial x}+\frac{\partial \vec{F}_v}{\partial y}\right)+\vec{S} \tag{1}$$

$$\begin{gathered}\vec{Q}=\begin{pmatrix}\rho\\ \rho u\\ \rho v\\ E_t\end{pmatrix},\quad \vec{E}=\begin{pmatrix}\rho u\\ \rho u^2+p\\ \rho uv\\ (E_t+p)u\end{pmatrix},\quad \vec{F}=\begin{pmatrix}\rho v\\ \rho vu\\ \rho v^2+p\\ (E_t+p)v\end{pmatrix}\\ \vec{E}_v=\begin{pmatrix}0\\ \tau_{xx}\\ \tau_{xy}\\ u\tau_{xx}+v\tau_{xy}+q_x\end{pmatrix},\quad \vec{F}_v=\begin{pmatrix}0\\ \tau_{xy}\\ \tau_{yy}\\ u\tau_{xy}+v\tau_{yy}+q_y\end{pmatrix}\end{gathered} \tag{2}$$

where:

$$\begin{aligned}q_x&=\frac{\gamma_\infty}{\mathrm{Pr}_\infty \mathrm{Re}(\gamma_\infty-1)}k\frac{\partial T}{\partial x}\\ q_y&=\frac{\gamma_\infty}{\mathrm{Pr}_\infty \mathrm{Re}(\gamma_\infty-1)}k\frac{\partial T}{\partial y}\end{aligned} \tag{3}$$

$$\begin{aligned}\tau_{xx}&=\frac{2}{3}\frac{\mu}{\mathrm{Re}}\left(2\frac{\partial u}{\partial x}-\frac{\partial v}{\partial y}\right)\\ \tau_{yy}&=\frac{2}{3}\frac{\mu}{\mathrm{Re}}\left(2\frac{\partial v}{\partial y}-\frac{\partial u}{\partial x}\right)\\ \tau_{xy}=\tau_{yx}&=\frac{\mu}{\mathrm{Re}}\left(\frac{\partial u}{\partial y}+\frac{\partial v}{\partial x}\right)\end{aligned} \tag{4}$$

S represents the source term for thermochemical phenomena or axisymmetric flow. Depending on the treatment of the reaction effect of air molecules, three types of gas can be considered.

To "close" the preceding system of equations, relations between the thermodynamic variables are required along with relations for the transport properties μ^* and k^*. For the present equilibrium flow computations, approximate curve fits are employed for thermodynamic and transport properties. The thermodynamic properties are obtained using the correlations developed by Tannehill and Mugge [11]:

$$a=a(\rho,e),\qquad T=T(\rho,e),\qquad p=p(\rho,e),\qquad h=h(\rho,e) \tag{5}$$

These curve fits are valid for temperatures up to 25000 K and density ratios (ρ^*/ρ_0^*) from 10^{-7} to 10^3. For both the equilibrium air and the perfect gas, the following relations between flow variables can be used:

$$p=\rho e(\gamma-1),\qquad E=\rho\left[e+\frac{1}{2}\left(u^2+v^2\right)\right],\qquad \gamma=\frac{h}{e} \tag{6}$$

The curve fits for the transport properties were developed by Srinivasan et al. [12] and include the following correlations:

$$k = k(\rho, e), \qquad \mu = \mu(\rho, e) \tag{7}$$

These curve fits are valid for temperatures up to 15000 K and density ratios (ρ/ρ_0) from 10^{-6} to 10^{1}.
For perfect-gas computations, $\gamma = \gamma_\infty$, the molecular viscosity μ is determined by the Sutherland law and the coefficient of thermal conductivity is calculated by assuming a constant Prandtl number, $\Pr = 0.72$.

Space Discretization

The Navier-Stokes equation neglecting the source term can be written as follows:

$$\frac{\partial}{\partial t}\iint_{\Omega} Q \ dV + \oint_{\partial\Omega} F(Q).\hat{n} \ dS = \oint_{\partial\Omega} G(Q).\hat{n} \ dS \tag{8}$$

where:

$$F(Q).\ \hat{n} = (V.\ \hat{n})\begin{Bmatrix} \rho \\ \rho u \\ \rho v \\ (E + p) \end{Bmatrix} + p\begin{Bmatrix} 0 \\ \hat{n}_x \\ \hat{n}_y \\ 0 \end{Bmatrix} \tag{9}$$

$$G(Q).\ \hat{n} = \vec{E}_v \hat{n}_x + \vec{F}_v \hat{n}_y \tag{10}$$

Here $\hat{n}_x$ and $\hat{n}_y$ are the Cartesian components of the exterior surface unit normal $\hat{n}$ on the boundary $\partial\Omega$.

The semi discrete form of the equations is as follows:

$$\frac{d}{dt}\left(Q_j A_j\right) + \sum_{k=1}^{nedge} \vec{F}_k dS_k = \sum_{k=1}^{nedge} \vec{G}_k dS_k \tag{11}$$

Inviscid Fluxes

A flux splitting scheme AUSMD has been constructed with an aim at removing numerical dissipation of the Van Leer-type flux vector splittings on a contact discontinuity. The obtained scheme is also recognized as an improved advection upstream splitting method (AUSM) by Liou and Steffen. The proposed scheme has the following favorable properties: accurate and robust resolution for shock and contact (steady and moving) discontinuities; conservation of enthalpy for steady flows; algorithmic simplicity; and easy extension to general conservation laws such as that for chemically reacting flows. Extensive numerical experiments were conducted to validate the proposed scheme for a wide range of problems, and the results are compiled for comparison with several recent upwind methods.

This scheme is referred to as the AUSMD since the numerical flux is similar in form to the FDS. In this scheme the interface flux is computed based on the following relation [10]:

$$F_k = \frac{1}{2}\left[(\rho U)_k (\psi_L + \psi_R) - \left|(\rho U)_k\right| (\psi_R - \psi_L)\right] + \vec{P}_k \tag{12}$$

where ψ is defined as follow:

$$\psi = \begin{pmatrix} 1 \\ u \\ v \\ H \end{pmatrix} \tag{13}$$

In this scheme the mass flux is computed based on the following relation:

$$(\rho U)_k = U_L^+ \rho_L + U_R^- \rho_R \tag{14}$$

In the above equation, U_L^+, U_R^- are selected so that having the best resolution in shock discontinuity and the following expressions are defined these parameters.

$$U_L^+ = \begin{cases} \alpha_L \left[\dfrac{(U_L + a_m)^2}{4a_m} \right] + (1-\alpha_L) \times \dfrac{U_L + |U_L|}{2} & \text{if } \ |U_L| \le a_m \\ \dfrac{U_L + |U_L|}{2} & \text{otherwise} \end{cases} \tag{15}$$

$$U_R^- = \begin{cases} \alpha_R \left[-\dfrac{(U_R - a_m)^2}{4a_m} \right] + (1-\alpha_R) \times \dfrac{U_R - |U_R|}{2} & \text{if } \ |U_R| \le a_m \\ \dfrac{U_R - |U_R|}{2} & \text{otherwise} \end{cases} \tag{16}$$

$\alpha_{L,R}$ are defined as follows:

$$\alpha_L = \frac{2(p/\rho)_L}{(p/\rho)_L + (p/\rho)_R} \tag{17}$$

$$\alpha_R = \frac{2(p/\rho)_R}{(p/\rho)_L + (p/\rho)_R} \tag{18}$$

Interface sound speed can be computed as follows:

$$a_m = Max(a_L, a_R) \tag{19}$$

The pressure flux is computed based on the following relation:

$$\vec{P}_k = p_k \begin{pmatrix} 0 \\ n_x \\ n_y \\ 0 \end{pmatrix} \tag{20}$$

where:

$$p_k = p_L^+ + p_R^- \tag{21}$$

The split pressures are calculated using the following relations:

$$p_L^+ = \begin{cases} p_L \dfrac{(U_L + a_m)^2}{4a_m^2}\left(2 - \dfrac{U_L}{a_m}\right) & if \quad |U_L| \le a_m \\ p_L \dfrac{U_L + |U_L|}{2U_L} & otherwise \end{cases} \tag{22}$$

$$p_R^- = \begin{cases} p_R \dfrac{(U_R - a_m)^2}{4a_m^2}\left(2 + \dfrac{U_R}{a_m}\right) & if \quad |U_R| \le a_m \\ p_R \dfrac{U_R - |U_R|}{2U_R} & otherwise \end{cases} \tag{23}$$

Viscous Fluxes

Viscous fluxes would be written as the followings [13]:

$$G(Q).\hat{n} = \begin{pmatrix} 0 \\ \tau_{xx} \\ \tau_{xy} \\ u\tau_{xx} + v\tau_{xy} + q_x \end{pmatrix}\hat{n}_x + \begin{pmatrix} 0 \\ \tau_{xy} \\ \tau_{yy} \\ u\tau_{xy} + v\tau_{yy} + q_y \end{pmatrix}\hat{n}_y \tag{24}$$

The viscous terms of Navier-Stokes equations are usually well behaved terms in computational manipulations. Due to their physical nature, a central difference scheme is usually appropriate in the discretization procedure of those terms. A special attention has to be made for calculation of u, v and T derivatives in unstructured grids. To resolve this problem following expression is proposed by Frink [13] based on Mitchell [14] works:

$$\begin{bmatrix} x_{c2} - x_{c1} & y_{c2} - y_{c1} \\ x_{n2} - x_{n1} & y_{n2} - y_{n1} \end{bmatrix}\begin{bmatrix} u_x \\ u_y \end{bmatrix} = \begin{bmatrix} u_{c2} - u_{c1} \\ u_{n2} - u_{n1} \end{bmatrix} \tag{25}$$

To implement this relation the data at the cell vertices should be computed based on the data stored at the cell center. Frink [15] proposed the following expression:

$$\vec{q}_n = \frac{\sum_{i=1}^{N} \dfrac{\vec{q}_{c,i}}{r_i}}{\sum_{i=1}^{N} \dfrac{1}{r_i}} \tag{26}$$

where:

$$r_i = \left[(x_{c,i} - x_n)^2 + (y_{c,i} - y_n)^2\right]^{\frac{1}{2}}, \qquad \vec{q} = \begin{pmatrix} \rho \\ u \\ v \\ p \end{pmatrix} \tag{27}$$

The subscripts n and c,i refer to the node and surrounding cell-centered values, respectively.

Boundary Conditions

Wall Boundary Condition

The application of the pseudo-Laplacian averaging to boundary nodes requires the implementation of ghost cells [16]. Ghost cells are produced by constructing an image cell across the exterior boundary of an adjacent interior cell. The geometric information is supplied by the following vector relations:

$$\begin{aligned} x_{gh} &= \left(x_{cj} - x_{nb}\right) - 2X\hat{n}_x \\ y_{gh} &= \left(y_{cj} - y_{nb}\right) - 2X\hat{n}_y \end{aligned} \tag{28}$$

where:

$$X = \left(x_{cj} - x_{nb}\right)\hat{n}_x + \left(y_{cj} - y_{nb}\right)\hat{n}_y \tag{29}$$

X is a contravariant vector component of distance, and the subscript nb denotes a boundary node.

The boundary conditions of u, v, p, T, ρ for Euler and Navier-Stokes equations can be expressed as follows:

$$\begin{cases} \begin{Bmatrix} u \\ v \end{Bmatrix}_{gh} = \begin{bmatrix} 1 - 2\hat{n}_x^2 & -2\hat{n}_x\hat{n}_y \\ -2\hat{n}_x\hat{n}_y & 1 - 2\hat{n}_y^2 \end{bmatrix} \begin{Bmatrix} u \\ v \end{Bmatrix}_j & Euler \quad Eq. \\ \begin{Bmatrix} u \\ v \end{Bmatrix}_{gh} = \begin{Bmatrix} -u \\ -v \end{Bmatrix}_j & Navier-Stokes \quad Eq. \end{cases} \tag{30}$$

$$\begin{aligned} & p_{gh} = p_j, \qquad E_{gh} = E_j \\ & \begin{cases} T_{gh} = T_j & Adiabatic \quad Wall \\ T_{gh} = T_{Const.} & Const. \ Temperature \quad Wall \end{cases} \end{aligned} \tag{31}$$

Farfield Boundary Condition

For supersonic inlet/outlet boundary condition, the flow variables at the boundary are those from upstream of the flow. So for supersonic inlet, all flow variables are those of the free stream, and for supersonic outlet, the flow characteristics are those from the adjacent interior cell.

Characteristic boundary conditions are applied to the far-field subsonic boundary using the fixed and extrapolated Riemann invariants corresponding to the incoming and outgoing waves. The incoming Riemann invariants are determined from the free stream flow and the outgoing invariants are extrapolated from the interior domain. The invariants are used to determine the locally normal velocity component and speed of sound. At an outflow boundary, the two tangential velocity components and the entropy are extrapolated from the interior, while at an inflow boundary they are specified as having farfield values. These five quantities provide a complete definition of the flow in the farfield.

Results

There are three test cases studied in this section. First, hypersonic laminar flow with equilibrium gas effects over flat plate. The free stream conditions are the same as those presented in [17] and as follows:

$$\begin{aligned} & M_\infty = 20.0, \quad P_\infty = 10.41Pa, \quad \rho_\infty = 3.626848 \times 10^{-4}\, kg/m^3 \\ & T_\infty = 100.0K, \quad \mu = 7.27 \times 10^{-6}\, kg/ms, \quad L = 1.0\, m \\ & \gamma = 1.4, \quad \Pr = 0.72, \quad T_{Wall} = 1000.0K \end{aligned}$$

As it is shown in fig. 1, the density decreases in the normal direction and then it arise. This is because of viscous interaction that occurs in boundary layer in hypersonic flow fields. This phenomena cause the temperature rise in the boundary layer. Furthermore, the pressure gradient in the normal direction to the flow field in the boundary layer is equal to zero. So the density should decrease near the boundary layer. In contrast, because of the growth of the boundary layer, a virtual wall appears in flow and an oblique shock occurs in the flow, so the density is increased behind it. The temperature and velocity profiles at exit plane and are presented in figs. 2 and 3 respectively, compared with corresponding results presented in ref. [17]. As it is obvious the presented results have good agreement with results presented in [17].

Second test case is a hypersonic laminar flow with equilibrium gas effects over wedge with 10 degree half angle. The free stream flow condition is the same as those presented in the first problem with the same flow conditions in [17].

The temperature and tangential velocity profile at exit plane are presented in figs. 6 & 7, respectively and are compared with results presented in Ref. [17].

As it is shown in Fig. 6 and 7 there are some oscillations behind an oblique shock in results presented in [17], but these are disappeared in the present work. The different value of maximum temperature obtained by the presented results with respect to that presented in Ref. [17] could be due to the first order approximation implemented in our simulation.

The last test case is hypersonic flow with equilibrium gas effects over blunt body. The free stream flow conditions are the same as those presented in [18] and as follows:

$$M_\infty = 11.26, \quad P_\infty = 2.089495\,Pa, \quad \rho_\infty = 3.993156\times10^{-5}\,kg/m^3$$

$$\mu = 6.11\times10^{-6}\,kg/ms, \quad T_\infty = 100.0\,K, \quad \gamma = 1.4$$

$$L = R_N = 0.5m, \quad \mathrm{Pr} = 0.72, \quad T_{Wall} = 1000.0\,K$$

As it is shown in figs. 8 and 9 this scheme does not exhibit any “carbuncle phenomena” and it is obvious that in the real gas case, γ is no longer be a constant and is varied as a function of temperature.

Conclusion

As it is shown in the result, this scheme able to predict flow properties in the boundary layer region such as pressure coefficient over the wall and skin friction coefficient accurately. Additionally, this scheme does not require any artificial dissipation terms and does not exhibit any oscillation near the shock. But it is very sensitive to the grid shapes and may cause “carbuncle phenomena”. To avoid this, grids with high aspect ratio is very effective.

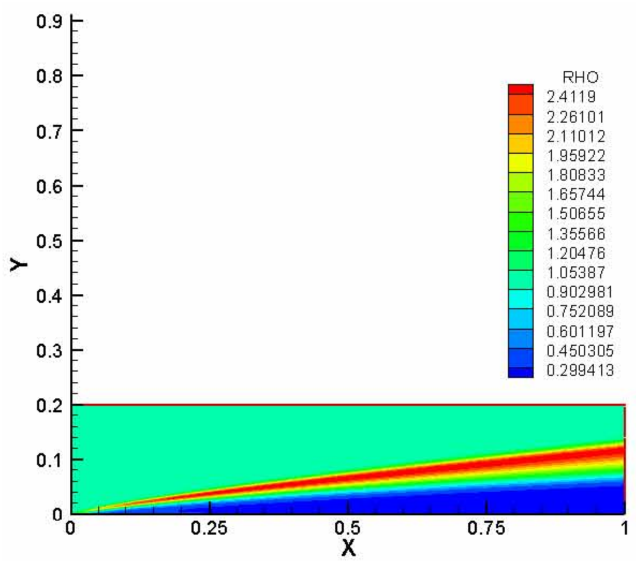

Fig. 1 The density contours over flat plate

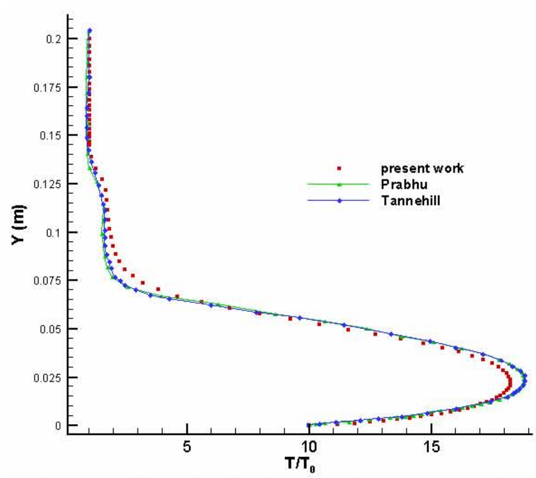

Fig. 2 Comparison of temperature profile at exit plane between present work and results presented in [17]

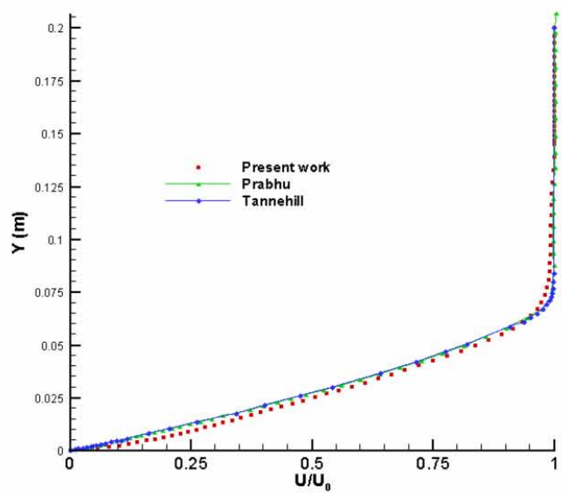

Fig. 3 Comparison of velocity profile at exit plane between present work and results presented in [17]

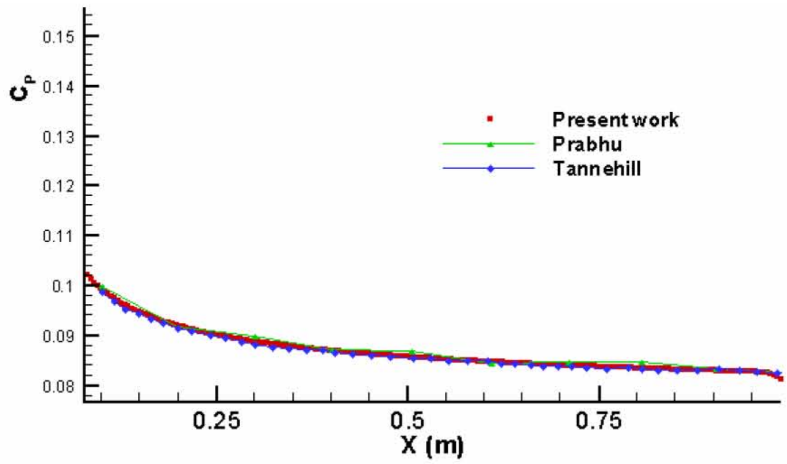

Fig. 4: The pressure coefficient over the wall

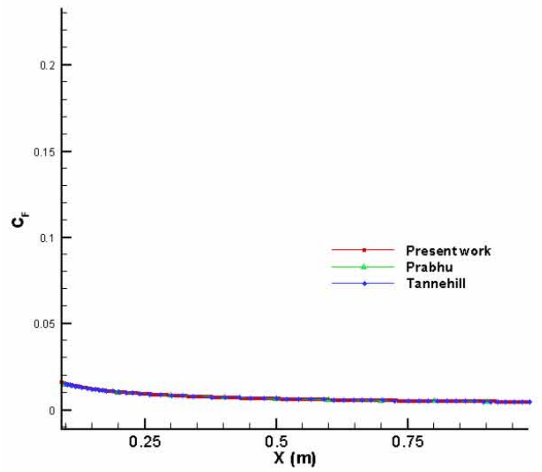

Fig. 5: The friction coefficient over the wall

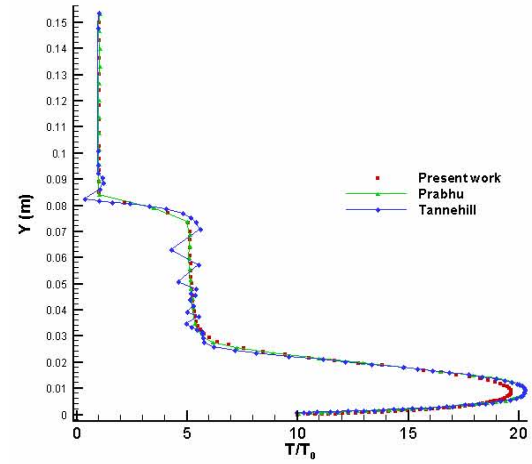

Fig. 6 Comparison of temperature profile at exit plane between present work and results presented in [17]

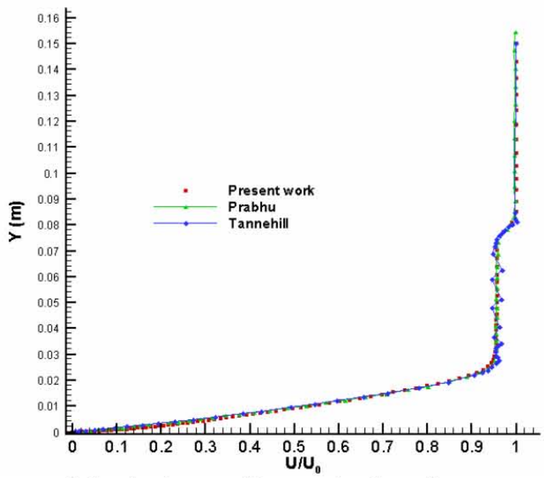

Fig. 7 Comparison of tangential velocity profile at exit plane between present work and results presented in [17]

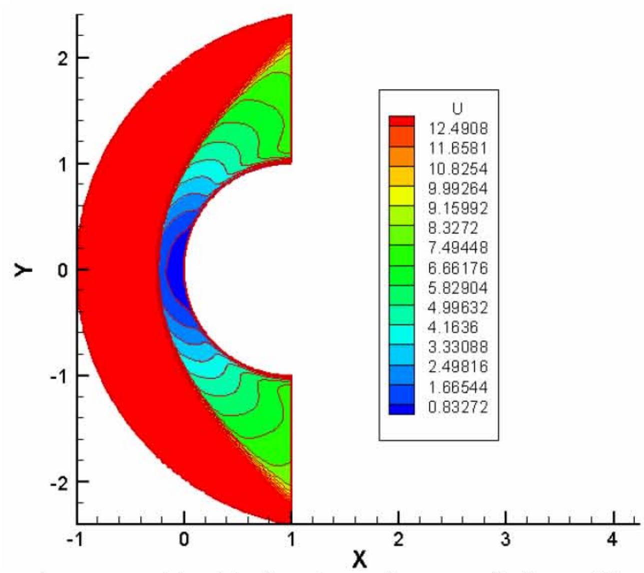

Fig. 8 The u velocity contours over blunt body, viscous hypersonic flow with equilibrium gas effects

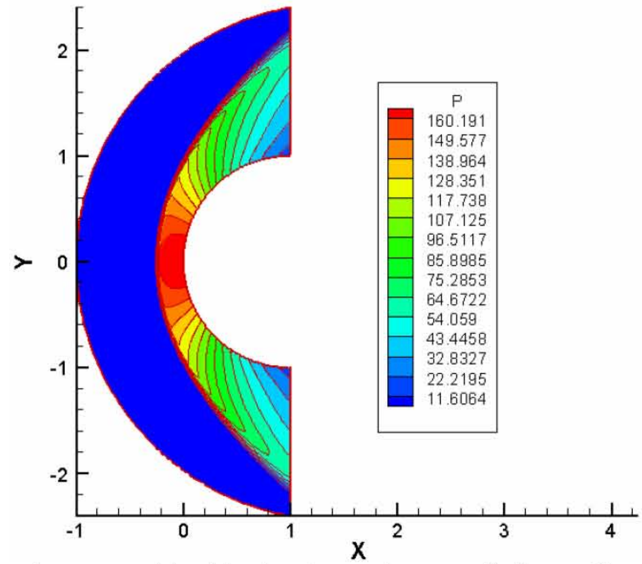

Fig. 9 The pressure contours over blunt body, viscous hypersonic flow with equilibrium gas effects

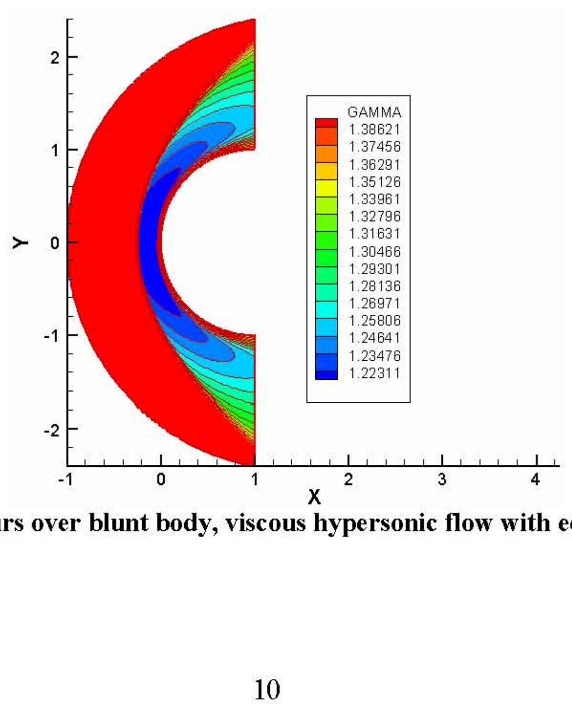

Fig. 10 The γ contours over blunt body, viscous hypersonic flow with equilibrium gas effects

References

[1]. Kim K. H., Kim C., Rho O. H., 2001, "Methods for the Accurate Computations of Hypersonic Flows, I. AUSMPW+ scheme", Journal of Computational Physics, 178, 38-80

[2]. K. H. Kim and C. Kim, "Accurate, efficient and monotic numerical methods for multi-dimensional compressible flows, Part I: Spatial discretization", J. Comput. Phys. 208 (2005), 527-569

[3]. Steger J. L. , Warming R. F., 1981, "Flux vector splitting of the inviscid gasdynamic equations with application to finite-difference methods", Journal of Computational Physics, 40, 263

[4]. Van Leer B., 1982, "Flux-vector splitting for the Euler equation", Lecture Notes Physics, 170, 507

[5]. Gressier J., Villedieu P., Moshetta J. M., 1999, "Positivity of flux vector splitting schemes", Journal of Computational Physics, 155, 199

[6]. Roe P. L., 1981, "Approximate Riemann solvers, parameter vectors and difference schemes", Journal of Computational Physics, 43, 357

[7]. Quirk J. J., 1994, "A contribution to the great Riemann solver debate", International Journal of Numerical Methods in Fluids, 18, 555

[8]. Einfeldt B., 1988, "On Godunov-type method for gas dynamics", *SIAM J. Numer Anal.* 25, No. 2, 294

[9]. Liou M. S., Steffen C. J., 1993, "A new flux splitting scheme", Journal of Computational Physics, 107, 23

[10]. Liou M. S., Wada Y., 1994, "A Flux Splitting Scheme with High-Resolution and Robustness for Discontinuities", AIAA Paper 94-0083, AIAA Press, Washington, DC

[11]. Tannehill, J. C. and Mugge T. L., "Improved Curve-Fits for the Thermodynamic Properties of Equilibrium Air Suitable for Numerical Computation Using Time Dependent or Shock-Capturing Methods," NASA CR-2470, 1974.

[12]. Srinivasan, S., Tannehill, J. C. and Weilmuenster, K. J., "Simplified Curve Fits for the Transport Properties of Equilibrium Air," NASA RP-1181, 1987.

[13]. N. T. Frink, (1996) "Assessment of an Unstructured Grid Method for Predicting 3D Turbulent Viscous Flows", AIAA-96-0292, 34th Aerospace Sciences Meeting, Reno, Nevada

[14]. C. R. Mitchell,(1994) "Improved Reconstruction Schemes for Navier-Stokes Equations on Unstructured Meshes.", AIAA Paper 91-0721, January 1994

[15]. N. T. Frink, Paresh Parikh, Shahryar Pirzadeh, "A Fast Upwind Solver for the Euler Equations on Three-Dimensional Unstructured Meshes", AIAA Paper 91-0102

[16]. N. T. Frink, "Recent Progress Toward a Three-Dimensional Unstructured Navier-Stokes Flow Solver", AIAA Paper 94-0061

[17]: J. C. Tannehill, J. O. Ievalts, S. L. Lawrence, "An Upwind Parabolized Navier-Stokes Code for Real Gas Flows", AIAA-88-0713, AIAA 26th Aerospace Sciences Meeting, 1988, Reno, Nevada

[18]. Vigneron, Y. C., (1976) "Hypersonic Viscous Flow of Equilibrium Air around a Blunt Body," M.S. Thesis, The Iowa State university, Iowa.